Biochemical and Biophysical Research Communications 386 (2009) 140–145

Contents lists available at ScienceDirect

Biochemical and Biophysical Research Communications

journal homepage: www.elsevier.com/locate/ybbrc

Tylophorine arrests carcinoma cells at G1 phase by downregulating cyclin A2 expression

Chia-Mao Wu [a], Cheng-Wei Yang [a], Yue-Zhi Lee [a], Ta-Hsien Chuang [b], Pei-Lin Wu [c], Yu-Sheng Chao [a], Shiow-Ju Lee [a,*]

[a] Division of Biotechnology and Pharmaceutical Research, National Health Research Institutes, Miaoli County 350, Taiwan, ROC
[b] College of Pharmacy, China Medical University, TaiChung 404, Taiwan, ROC
[c] Department of Cosmetic Science, Chung Hwa College of Medical Technology, Tainan 717, Taiwan, ROC

ARTICLE INFO

Article history:
Received 27 May 2009
Available online 6 June 2009

Keywords:
Carcinoma cells
Cyclin A2
G1 arrest
Phenanthroindolizidine
Tylophora
Tylophorine

ABSTRACT

Tylophorine, a representative phenanthroindolizidine alkaloid from *Tylophora indica* plants, exhibits anti-inflammatory and anti-cancerous growth activities. However, the underlying mechanisms of its anti-cancer activity have not been elucidated and its effects on cell cycle remain ambiguous. Here, we reveal by asynchronizing and synchronizing approaches that tylophorine not only retards the S-phase progression but also dominantly arrests the cells at G1 phase in HepG2, HONE-1, and NUGC-3 carcinoma cells. Moreover, tylophorine treatment results in down regulated cyclin A2 expression and overexpressed cyclin A2 rescues the G1 arrest by tylophorine. Thus, we are the first to report that the downregulated cyclin A2 plays a vital role in G1 arrest by tylophorine in carcinoma cells.

Introduction

Tylophorine belongs to the small group of plant natural compounds, phenanthroindolizidine alkaloids, which have recently been exploited as potential cancer therapy drugs because of their high potency against various cancer cell lines [1–10]. In the 1960s, trials of tylocrebrine as an anti-cancer agent were discontinued because of central-nervous-system side effects [11]. Therefore, effort has been invested in molecular pharmacology studies [8,12,13] and improving the physical properties, such as polarity and hydrophilicity, of this group of compounds to avoid drug transfer through the blood–brain barrier [2,14].

Cyclin-dependent kinases (CDKs) and cyclins play critical roles in cell cycle regulation [15,16]. Many anti-cancer agents derived from natural products exhibit growth inhibitory activity in carcinoma cells through cell cycle regulation. For instance, paclitaxel inhibits microtubule disassembly, and butyrolactone inhibits CDK activity; both cause cell cycle arrest at the G2/M phase [17,18]. Antofine, a tylophorine analogue, arrests the cell cycle at the G2/M phase in Col2, human colon cancer cells [19]. DCB3500 (tylophorine) and DCB3503 (a tylophorine analogue) cause S-phase accumulation of KB cells but have no effect on specific cell cycle arrest in HepG2 cells [8]. DCB3503's effect on cell cycle progression was further examined in PANC-1 cells [13] and was suggested to be through downregulated cell cycle regulatory proteins. However, more information on specific interactions and relations is needed to elucidate substantial links between phenanthroindolizidine alkaloids and anti-cancer-cell growth and cell cycle interference.

Here, we unravel the effect of tylophorine on cancer cell cycle specific interference and the involvement of downregulated cyclin A2 in anti-cancer cell growth mechanisms of tylophorine.

Materials and methods

Cell culture and reagents. HepG2 (HB-8065; ATCC), HONE-1 [20] (a gift from Dr. Ching-Hwa Tsai at National Taiwan University, Taiwan, ROC) and NUGC-3 cells (the Japanese Cancer Research Resources Bank) were maintained in DMEM (Hyclone Inc.) supplemented with 10% heat inactivated fetal calf serum (Biological Industries Inc.) and penicillin–streptomycin (BioSource, Invitrogen) in a 5% CO_2 atmosphere at 37 °C in a humidified incubator. Tylophorine was prepared as described, as was dehydro-tylophorine, with modification [21]; dehydro-tylophorine was prepared by reacting tylophorine with *N*-bromosuccinimide and then exposure under light. The final product was verified by liquid chromatography/mass spectrometry (Agilent Technologies), with no

* Corresponding author. Address: No. 35, Keyan Road, Zhunan Town, Miaoli County 350, Taiwan, ROC. Fax: +886 37 586456.
E-mail address: slee@nhri.org.tw (S.-J. Lee).

0006-291X/$ - see front matter © 2009 Elsevier Inc. All rights reserved.
doi:10.1016/j.bbrc.2009.05.138

tylophorine detected (data not shown). HPLC-degree dimethyl sulfoxide (DMSO), nocodazole, thymidine, propidium iodide and BrdU were purchased from Sigma–Aldrich.

Cell synchronization procedures were as follows. For double-thymidine blocking, cells growing exponentially were incubated with 2 mM thymidine-containing DMEM complete medium for two sequential 18 h periods, with a 10 h recovery period without thymidine between the 18 h periods. For thymidine-nocodazole blocking, cells growing exponentially were incubated with 2 mM thymidine-containing complete medium for 18 h, then the medium was replaced with one containing 50 ng/ml nocodazole for 8 h incubation before compound treatment. For serum starvation, cells were cultured in medium containing 0.5% FCS for 48 h before compound treatment in DMEM complete medium.

Cell growth inhibition assay. Concentrations for 50% growth inhibitory effect, GI_{50} values, measured for HepG2, HONE-1 and NUGC-3 cells were determined as described [22]. For drug removal experiments, HepG2, HONE-1 and NUGC-3 cells were seeded at 5000, 2500, and 3000 cells/well respectively in 24-well plates. After 24 h, cells were treated with drugs for another 24 h. The drug-containing medium was then removed (day 0), and cells were incubated in drug-free medium for another 1–8 days. At the end of each incubation period, the number of viable cells was estimated by MTS assay [22].

Western blot analysis. Whole cell lysates were prepared with use of PRO-PREP™ protein extraction solution (iNtRON Biotechnology) and quantitated by BCA protein assay (Pierce Biotechnology). Equal amounts of protein per lane were subjected to SDS–PAGE, transferred to nitrocellulose membranes, and immunoblotted with antibodies against cyclin A2, cyclin B1, Cdk1 (Santa Cruz Biotechnology), p27, cyclin E, Cdk2 (Abcam), Cdk4 (Cell Signaling), tubulin (Amersham Life Science), and horseradish peroxidase-conjugated secondary antibodies (PerkinElmer). Detection of antigen–antibody complexes involved ECL detection reagents (Western Blot Chemiluminescence Reagent Plus, PerkinElmer), according to the manufacturers' instructions.

Plasmid construction, transfection and luciferase assay. The human cyclin A2 was amplified from the MGC 132447 clone (Open Biosystems) by use of 5′-CGAATTCCGATGTTGGGCAACTCTGCG-3′ and 5′-GCCTCGAGTTACAGATTTAGTGTCTCTGGTGG-3′, then subcloned into EcoRI/XhoI sites of pCMV-myc (Clontech) to generate the CCNA2-pCMV-myc expression vector. The human cyclin A2 promoter region (fragment from −215 to +245) was amplified from a BAC clone RP11-63B12 (Invitrogen) by PCR and subcloned into a SacI/SmaI site of the pGL3basic luciferase reporter vector (Promega) to create a cyclin A2 promoter-driven luciferase reporter gene construct, pCCNA2-pGL3basic. The sequences of all constructs were verified by DNA sequencing. FuGene 6™ (Roche) and the Steady-Glo luciferase assay system (Promega) were used for transient transfection and luciferase activity assay according to the manufacturers' instructions [12]. The luciferase activity was normalized to protein concentration and presented as relative activity compared to vehicle (0.1% DMSO) control.

Cell cycle analysis. Cells were trypsinized, washed twice with PBS and fixed in 70% ethanol at 4 °C for at least 1 h. Fixed cells were centrifuged and resuspended in 50 μg ml^{-1} RNase and 10 μg ml^{-1} propidium iodide for DNA staining at 37 °C for 1 h. DNA content was measured by use of a FACS flow cytometer (BD Biosciences). DNA histograms were obtained by use of ModFit LT 3.1 (Verity Software House, Topsham, ME). Cell aggregates were gated by analysis, and each profile was compiled from at least 10,000 gated events.

For cyclin A2-myc over-expression experiments, HONE-1 cells were transfected with pCMV-myc or CCNA2-pCMV-myc expression vectors the day before treated with DMSO or 2 μM tylophorine in the presence of nocodazole (25 ng/ml) for further 24 h, respectively. After compound treatment, cells were harvested and fixed by 70% ethanol, then incubated with the monoclonal anti-myc tag antibody (Santa Cruz Biotechnology) in staining solution (1% BSA, 0.1% Triton X-100 in PBS) for 1 h at RT. After being stained, cells were washed by staining solution twice and resuspended in staining solution containing FITC-conjugated anti-mouse IgG antibody (Santa Cruz Biotechnology) and incubated at RT for 30 min. After being washed, the resulting cells were stained with propidium iodide for DNA as mentioned previously. The FITC signal and propidium iodide were detected in FL-1 and FL-2 channels, respectively, by BD FACS flow cytometry. More than 10,000 FITC-positive cells were gated for cell cycle analysis.

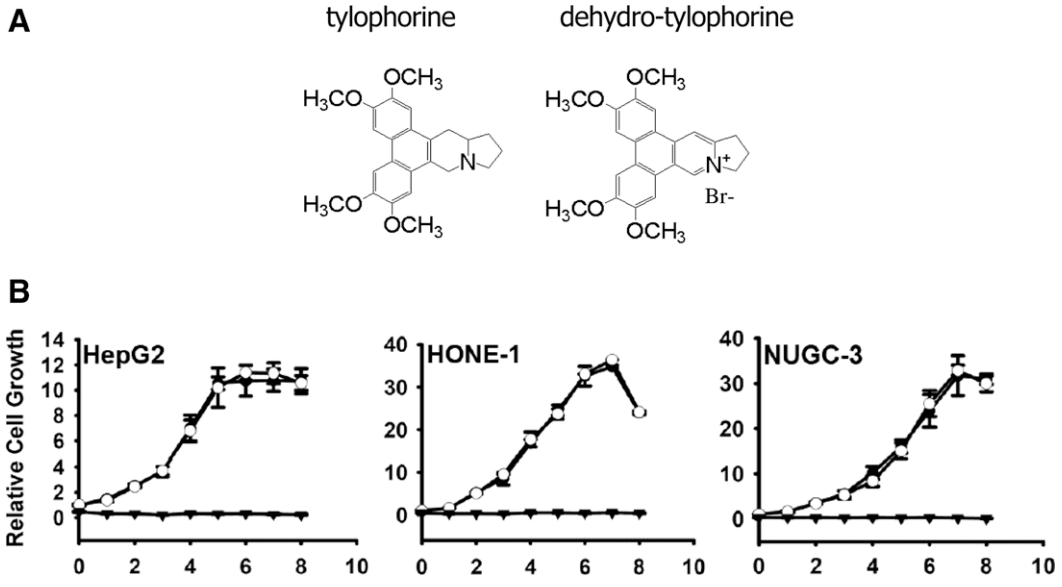

Fig. 1. Effect of tylophorine and dehydro-tylophorine on the growth of carcinoma cells. (A) Chemical structures of synthesized tylophorine and dehydro-tylophorine. (B) Tylophorine irreversibly inhibited the growth of carcinoma cells. Cells were seeded one day before treatment with vehicle (0.2% DMSO, (●), 2 μM dehydro-tylophorine (○), or 2 μM tylophorine (▼) for 24 h. The drug-containing medium was then removed (day 0), and the cells were incubated in drug-free medium for another 1–8 days. Data are representative of three independent experiments and are means ± SD of triplicate samples.

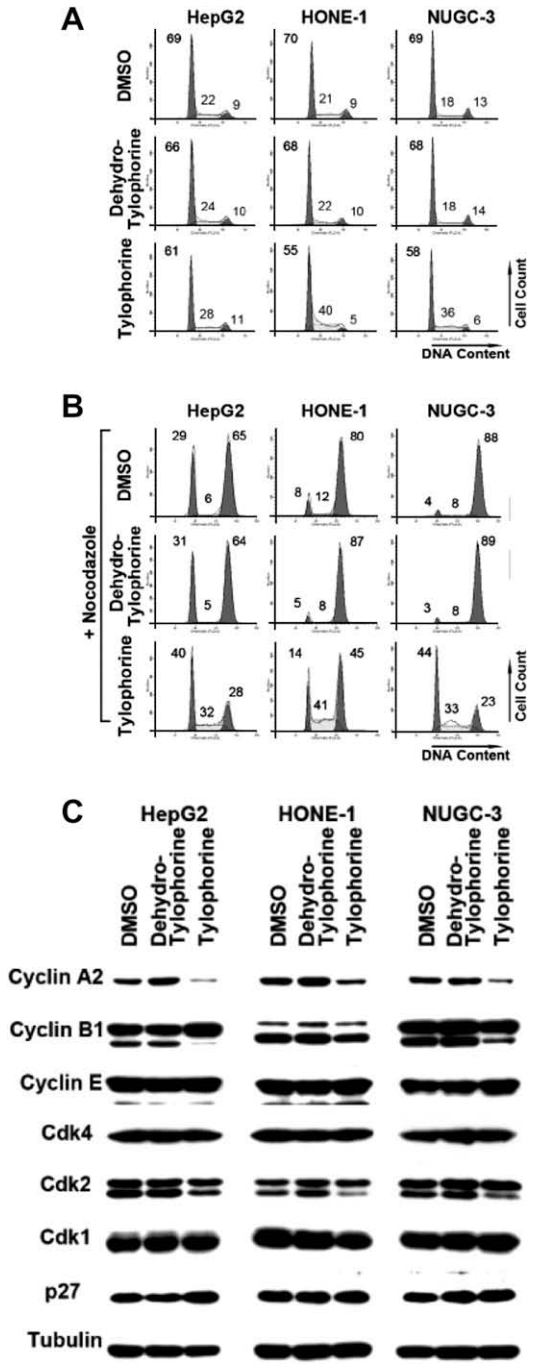

Fig. 2. Effect of tylophorine on cell cycle progression in asynchronized carcinoma cells. (A) Proportion of cells in S-phase accumulated with tylophorine treatment. Cells were seeded one day before treatment with vehicle (0.1% DMSO), 2 μM dehydro-tylophorine, or 2 μM tylophorine for 24 h, stained with propidium iodide, then analyzed by flow cytometry. (B) Proportions of cells in G1 and S-phases accumulated with tylophorine cotreament with nocodazole. Cells were co-treated with 25 ng/ml nocodazole and compounds for 24 h and processed as described in (A). The proportions of cells in G1, S and G2/M phases are indicated. (C) Western blot analysis of effect of tylophorine on cell cycle regulatory protein expression. Protein levels of cyclins (cyclin A2, cyclin B1, and cyclin E), cyclin-dependent kinases (Cdk4, Cdk2 and Cdk1), p27, and the loading control, tubulin, in cells after treatment as described in (A) were analyzed. Shown are representative results of three independent experiments.

Results

Tylophorine inhibits carcinoma cell growth

To examine whether tylophorine is cytotoxic or inhibits carcinoma cell growth, we performed a drug removal experiment in addition to growth inhibition assays to determine the concentrations for 50% growth inhibition (GI_{50}). As a negative control, a least-active tylophorine analogue, dehydro-tylophorine, was studied [4] (Fig. 1A). Tylophorine, 2 μM, greatly inhibited the growth of HepG2, HONE-1 and NUGC-3 cells, with GI_{50} values (means ± S.D.) of 237 ± 32, 114 ± 6, and 134 ± 9 nM, respectively, whereas dehydro-tylophorine, 50 μM, had a slight effect—~13%, ~11%, and ~9% inhibition, respectively. With tylophorine treatment removed, HepG2, HONE-1, and NUGC-3 cells could not restore their capacity for growth up to 8 days later (Fig. 1B). Although most of tylophorine-treated cells were viable for 8 days, as seen on microscopy (data not shown) and MTS assay, their proliferation was completely blocked. In contrast, vehicle control (DMSO) and dehydro-tylophorine treatments did not affect the carcinoma cell growth and exponential proliferation.

Effect of tylophorine on cell cycle progression in asynchronized cells

We used a cell asynchronized approach to investigate the effect of the anti-cancer agent tylophorine on the cell cycle. Flow cytometry analyses with asynchronized cells revealed an accumulation of HONE-1 and NUGC-3 cells but not HepG2 cells in the S phase after 24-h incubation with 2 μM tylophorine as compared with DMSO and dehydro-tylophorine treatment (Fig. 2A). Tylophorine treatment resulted in about a 2-fold increase in cells in the S phase, ~21% to ~40% for HONE-1 cells and ~18% to ~36% for NUGC-3 cells.

When cells were co-treated with nocodazole, a G2/M blocker, the effect on the accumulation of cells in the S phase caused by tylophorine became more evident, with a 4- to 6-fold increase in cells in the S phase in all HepG2, HONE-1, and NUGC-3 lines as compared with co-treatment with DMSO and dehydro-tylophorine (Fig. 2B). In addition, co-treatment with tylophorine and nocodazole increased the number of cells in the G1 phase, with increases of 0.3- to 13.7-fold as compared with co-treatment with DMSO or dehydro-tylophorine. For example, the proportion of HepG2 cells in the G1 phase with nocodazole treatment alone was ~29% and increased to ~40% with nocodazole and tylophorine cotreament; in HONE-1 cells, the proportion increased from ~8% to ~14% and in NUGC-3 cells, from ~4% to ~44%.

We then examined the protein expression of cyclin A2, cyclin B1, cyclin E, Cdk1, Cdk2, Cdk4, and p27 (Fig. 2C). In asynchronized HepG2, HONE-1, and NUGC-3 cells, cyclin A2 level was significantly lower with tylophorine treatment than with DMSO and dehydro-tylophorine treatment. All three cell lines showed a slight decrease in cyclin B1 and Cdk2 level, whereas the level of the other proteins did not change significantly.

Tylophorine treatment reveals the G1 arrest in synchronized cells

HepG2, HONE-1, and NUGC-3 cell lines were synchronized by double-thymidine and thymidine-nocodazole blocking for G1/S and G2/M arrest, respectively, then released for cell cycle re-progression with or without tylophorine treatment.

When cells were released from G1/S arrest after double-thymidine treatment, cells at the G1/S transition proceeded to the S phase and then progressed slowly, with S-phase retardation in all three cell lines. Moreover, treatment with tylophorine at 48 and 72 h resulted in arrested cell cycle progression at the G1 phase (Fig. 3A). This G1 phase arrest was greater in thymidine-nocodazole synchronized cells, with a population in the G1 phase ranging from 45% to 79% at 48 and 72 h (Fig. 3B). Cells released from G2/M entered G1 but failed to progress to the S phase at 24, 48, and 72 h in all three cell lines. The increased number of cells in the G1 phase with incubation time indicated that cells progressing from S or G2/M and then entering G1 were dominantly arrested at G1. The slight decrease in number of cells in the S phase

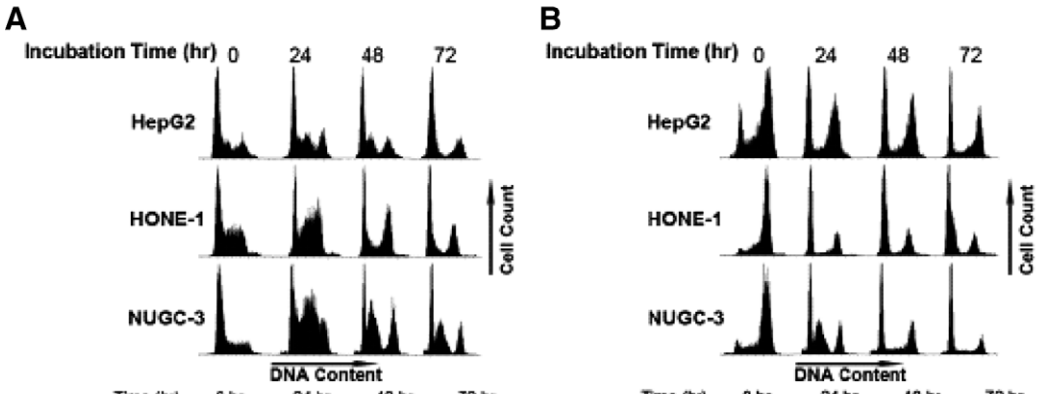

	Time (hr)	0 hr	24 hr	48 hr	72 hr
HepG2	G1	53 ± 1	42 ± 14	51 ± 3	77 ± 2
	S	43 ± 4	50 ± 16	37 ± 2	17 ± 6
	G2/M	4 ± 3	8 ± 3	12 ± 4	6 ± 4
HONE-1	G1	42 ± 10	14 ± 4	35 ± 3	55 ± 8
	S	58 ± 10	78 ± 6	48 ± 3	28 ± 2
	G2/M	0	8 ± 8	17 ± 4	17 ± 10
NUGC-3	G1	66 ± 6	20 ± 7	45 ± 11	56± 9
	S	34 ± 6	79 ± 5	33 ± 9	19 ± 3
	G2/M	0	1 ± 2	22 ± 3	24 ± 11

	Time (hr)	0 hr	24 hr	48 hr	72 hr
HepG2	G1	12 ± 5	43 ± 8	45 ± 11	57 ± 2
	S	37 ± 13	30 ± 7	34 ± 3	26 ± 8
	G2/M	54 ± 20	27 ± 14	25 ± 9	21 ± 5
HONE-1	G1	1 ± 1	66 ± 4	71 ± 1	79 ± 8
	S	27 ± 5	18 ± 7	18 ± 7	13 ± 1
	G2/M	72 ± 6	16 ± 11	11 ± 7	10 ± 5
NUGC-3	G1	3 ± 5	59 ± 10	70 ± 6	73± 7
	S	23 ±8	22 ± 4	18 ± 4	17 ± 4
	G2/M	74 ±12	19 ± 8	12 ± 2	10 ± 3

Fig. 3. G1 arrest with tylophorine treatment in synchronized carcinoma cells. Cells were synchronized by use of double thymidine for G1/S blocking (A) or thymidine-nocodazole for G2/M blocking (B), then released in medium containing 2 μM tylophorine and incubated for various times, stained with propidium iodide, then analyzed by flow cytometry. Shown are representative histograms of three independent experiments and mean ± S.D. of three independent experiments.

indicated that the progression of the S phase was retarded, and cells slowly progressed to G2/M and then G1, which resulted in the slight decrease in the number in the G2/M phase after being released for 24–72 h. Therefore, tylophorine inhibited carcinoma cell growth and proliferation by dominantly arresting cells at the G1 phase and retarding the S-phase progression.

Tylophorine decreases cyclin A2 expression through transcriptional regulation

Since the protein level of cyclin A2 was decreased in all three asynchronized cell lines with tylophorine treatment (Fig. 2C) and cyclin A2 is important for G1/S-phase transition and because tylophorine caused G1 phase arrest in synchronized cells, we examined cyclin A2 expression in synchronized cells. With DMSO or dehydro-tylophorine treatment in HepG2, HONE-1 and NUGC-3 cells, cyclin A2 protein level increased in the first 4–8 h after cells were released from double-thymidine block for G1/S arrest and then declined over time; however, with tylophorine treatment, 2 μM, cyclin A2 protein level declined linearly over 24 h (Fig. 4A). After release from serum starvation for G0/G1 arrest, with tylophorine treatment, the mRNA level of cyclin A2 was significantly lower than that with DMSO or dehydro-tylophorine treatment in all three cell lines, although the level was lower in NUGC-3 cells than in HepG2 and HONE-1 cells (Fig. 4B).

Furthermore, we used a cyclin A2 promoter-driven luciferase reporter gene construct, pCCNA2-pL3basic, to dissect the effect of tylophorine on cyclin A2 promoter activity. DMSO and dehydro-tylophorine had no significant effect on cyclin A2 promoter activity, whereas with 2 μM tylophorine, cyclin A2 promoter activity declined by more than 90% in all three cell lines (Fig. 4C). Thus, tylophorine is suggested to downregulate cyclin A2 expression through transcription.

Overexpression of cyclin A2 rescued the G1 arrest induced by tylophorine

In order to confirm the role of the decreased cyclin A2 expression in the G1 arrest caused by tylophorine treatment, we performed a gain-of-function experiment using transient expression of cyclin A2 protein in HONE-1 cells (Table 1). Cells transiently transfected with cyclin A2 for 24 h were treated with DMSO or tylophorine in the presence of nocodazole for 24 h before subject to cell cycle analysis. The cell population was divided into two groups, one with basal cyclin A2 expression level and the other with cyclin A2 overexpression (data not shown).

On one hand, cells with basal levels of cyclin A2 showed a significant increase in G1 population in the presence of tylophorine (21.68 ± 2.84%) compared DMSO treatment (7.58 ± 3.68%) for 24 h. Nonetheless, cells with overexpressed cyclin A2 exhibited a moderate decrease in G1 population by tylophorine treatment (5.05 ± 3.08%) compared to DMSO treatment (9.62 ± 3.13%). On the other hand, the trend of S-phase retardation by tylophorine treatment was not affected either in cells with basal or overexpressed cyclin A2 compared to respective DMSO treatment, 49.27 ± 9.56–19.33 ± 5.45% and 62.12 ± 5.55–31.33 ± 8.97%. Thus, overexpressed cyclin A2 rescued the G1 arrest but not S-phase retardation by tylophorine.

Discussion

Our treatment with cell cycle synchronizing agents unambiguously revealed that tylophorine interferes with the cell cycle through a dominant G1 arrest and retardation of the S-phase progress in HepG2, HONE-1, and NUGC-3 carcinoma cells. The retardation in the S-phase progression was delayed for 48 h or longer (Fig. 3A) and thus masked the G1 arrest in asynchronizing cells (Fig. 2A), as was found by others [8,13]. In addition, the tylophorine inhibited DNA synthesis (data not shown) is suggested to be associated with the S-phase retardation. The tylophorine-induced G1 phase arrest was difficult to pass through, as was strongly evident by the increased proportion of cells in the G1 phase and slightly decreased proportion in the S and G2/M phase with time after release from G2/M arrest by thimidine-nacodazole (Fig. 3B). Thus, the dominant inhibitory effect of tylophorine for carcinoma cell growth is the arrested G1 phase rather than the retarded S-phase progression (Fig. 3A and B).

Cyclin A2 is a cell cycle regulatory protein which gene expression is repressed during the G1 phase and induced at S-phase entry in non-transformed cells [23]. Ectopically expressed cyclin A2

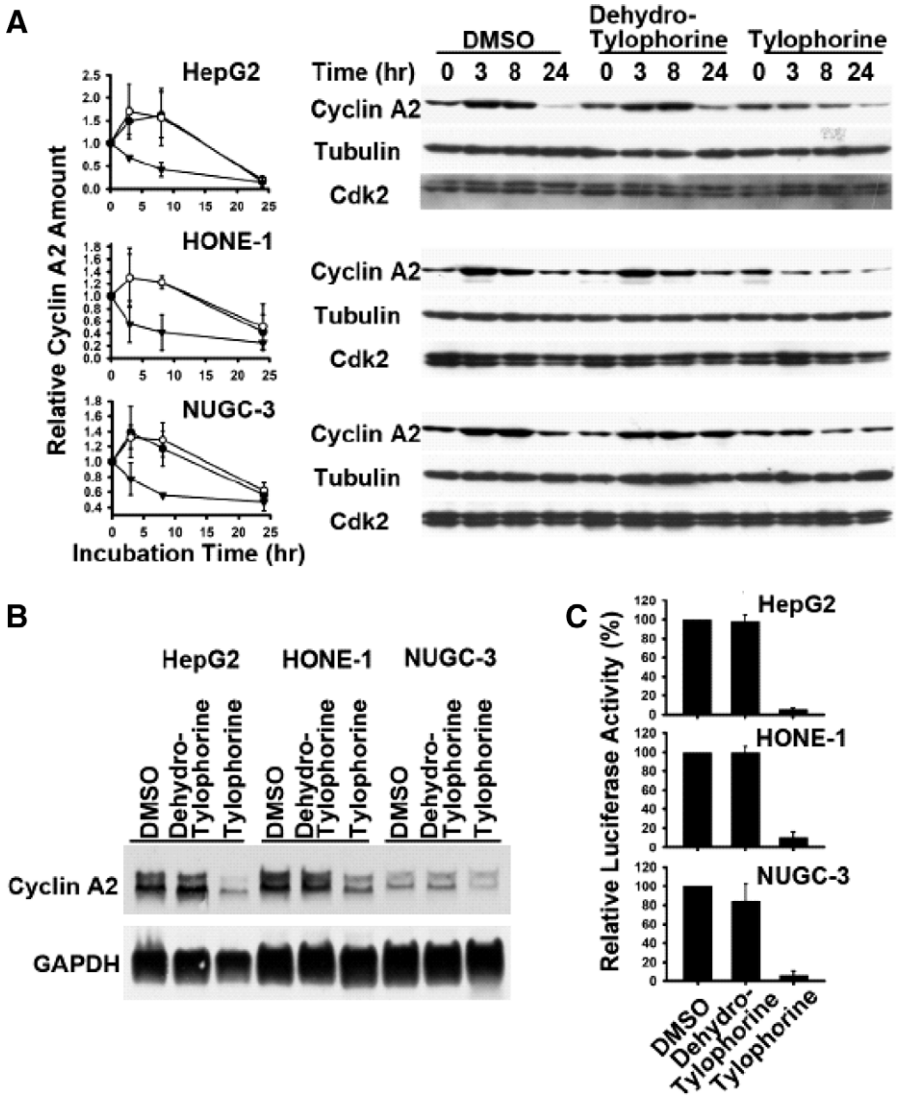

Fig. 4. Effect of tylophorine on cyclin A2 expression. (A) Western blot analysis of tylophorine inhibiting cyclin A2 protein expression. Cells were serum starved for 48 h then incubated with medium containing 10% FCS and compounds, and cells were harvested at various times. Data are mean ± S.D. of three independent experiments. Normalization was to level of tubulin. (B) Northern blot analysis of tylophorine-inhibited cyclin A2 mRNA expression. Cells were treated as described in (A). The filters were also hybridized with the DIG-labeled GAPDH probe for an internal loading control. Shown are representative of three independent experiments. (C) Tylophorine inhibited cyclin A2 promoter activity. Cells were transfected in suspension for 1 h with 1 μg of human cyclin A2 promoter luciferase reporter, pCCNA2-pGL3basic, and incubated for 20 h before compound treatment. Cells were treated with 0.1% DMSO (vehicle), 2 μM dehydro-tylophorine, or 2 μM tylophorine for a further 24 h, then luciferase activity was analyzed. The luciferase activity was normalized to protein concentration. Data are means ± S.D. of three independent experiments.

Table 1
Ectopically overexpressed cyclin A2 rescued G1 arrest with tylophorine treatment in HONE-1 cells. HONE-1 cells were transfected by CCNA2-pCMV-myc vectors as indicated for 24 h and then co-treated with nocodazole and vehicle (0.1% DMSO) or 2 μM tylophorine for 24 h, stained with propidium iodide and anti-myc tag antibody with FITC-conjugated IgG, and then underwent flow cytometry analysis. Shown are the means ± S.D. of three independent experiments for proportions of cells in G1, S and G2/M phases gated by overexpressed (high level) and basal level of cyclin A2.

		–	DMSO + Nocodazole	Tylophorine + Nocodazole
	Cyclin A2 level	0 h	24 h	24 h
G1	Basal	47.97 ± 4.68	7.58 ± 3.68(*1)	21.68 ± 2.84(*1)
	High	32.39 ± 1.29	9.62 ± 3.13(*2)	5.05 ± 3.08(*2)
S	Basal	34.14 ± 1.77	19.33 ± 5.45	49.27 ± 9.56
	High	67.61 ± 1.29	31.33 ± 8.97	62.12 ± 5.55
G2/M	Basal	17.89 ± 2.92	73.09 ± 7.82	29.05 ± 11.17
	High	0.00 ± 0.00	59.05 ± 11.20	32.82 ± 7.17

p.s. DMSO versus tylophorine treatments, (*1) and (*2) p values <0.05.

overcomes G1 arrest in confluent cultures [24] and the induced expression of cyclin A2 via JunD releases the cell contact inhibition (G1 arrest) upon the TCDD treatment in rat liver oval cells [24]. Our results suggest that downregulated cyclin A2 is involved in the tylophorine-induced G1 arrest in carcinoma cells since overexpressed cyclin A2 was able to overcome the tylophorine-induced G1 arrest and facilitated the S-phase entry. Moreover, overexpressed cyclin A2 did not play a significant role for overcoming the S-phase

retardation by tylophorine treatment, since the incremental trend of S-phase proportion remained the same in cells with basal or overexpressed cyclin A2 (Table 1). These results reflect the role of cyclin A2 in entry from G1 to S-phase [23].

Collectively, phenanthroindolizidines (e.g. tylophorine, antofine, and DCB3503) exhibit anti-cancer growth activity through interfering cell cycle progress but the detail effective cell cycle points and underlying mechanisms are suggested to be differentiated. In conclusion, we have clarified the effective points of tylophorine in carcinoma cell cycle progress and thus warrant further studies on the detail mechanisms of action. This study lays the foundation for future development of tylophorine analogues for anti-cancer therapeutic agents.

Acknowledgments

This work was supported by National Health Research Institutes, Taiwan, ROC [Grants BP-094-PP-04; BP-095-PP-04; BP-096-PP-05; BP-097-PP-05] and the National Science Council of Taiwan, ROC [Grant 95-320-B-400-010-MY3]. We appreciate support from the flow cytometry core facility at National Health Research Institutes. Mr. Cheng-Wei Yang is currently a Ph.D. student of the Graduate Program of Biotechnology in Medicine sponsored by the National Tsing Hua University and the National Health Research Institutes.

References

[1] H. Komatsu, M. Watanabe, M. Ohyama, T. Enya, K. Koyama, T. Kanazawa, N. Kawahara, T. Sugimura, K. Wakabayashi, Phenanthroindolizidine alkaloids as cytotoxic substances in a Danaid butterfly, Ideopsis similis, against human cancer cells, J. Med. Chem. 44 (2001) 1833–1836.
[2] L. Wei, Q. Shi, K.F. Bastow, A. Brossi, S.L. Morris-Natschke, K. Nakagawa-Goto, T.S. Wu, S.L. Pan, C.M. Teng, K.H. Lee, Antitumor agents 253. Design, synthesis, and antitumor evaluation of novel 9-substituted phenanthrene-based tylophorine derivatives as potential anticancer agents, J. Med. Chem. 50 (2007) 3674–3680.
[3] Z. Li, Z. Jin, R. Huang, Isolation, total synthesis and biological activity of phenanthroindolizidine and phenanthroquinolizidine alkaloids, Synthesis 16 (2001) 2365–2378.
[4] C.W. Yang, T.H. Chuang, P.L. Wu, W.H. Huang, S.J. Lee, Anti-inflammatory effects of 7-methoxycryptopleurine and structure-activity relations of phenanthroindolizidines and phenanthroquinolizidines, Biochem. Biophys. Res. Commun. 354 (2007) 942–948.
[5] Y. Fu, S.K. Lee, H.Y. Min, T. Lee, J. Lee, M. Cheng, S. Kim, Synthesis and structure-activity studies of antofine analogues as potential anticancer agents, Bioorg. Med. Chem. Lett. 17 (2007) 97–100.
[6] A.G. Damu, P.C. Kuo, L.S. Shi, C.Y. Li, C.S. Kuoh, P.L. Wu, T.S. Wu, Phenanthroindolizidine alkaloids from the stems of Ficus septica, J. Nat. Prod. 68 (2005) 1071–1075.
[7] X. Huang, S. Gao, L. Fan, S. Yu, X. Liang, Cytotoxic alkaloids from the roots of Tylophora atrofolliculata, Planta Med. 70 (2004) 441–445.
[8] W. Gao, W. Lam, S. Zhong, C. Kaczmarek, D.C. Baker, Y.C. Cheng, Novel mode of action of tylophorine analogs as antitumor compounds, Cancer Res. 64 (2004) 678–688.
[9] D. Staerk, J. Christensen, E. Lemmich, J.O. Duus, C.E. Olsen, J.W. Jaroszewski, Cytotoxic activity of some phenanthroindolizidine N-oxide alkaloids from Cynanchum vincetoxicum, J. Nat. Prod. 63 (2000) 1584–1586.
[10] K.N. Rao, S.R. Venkatachalam, Inhibition of dihydrofolate reductase and cell growth activity by the phenanthroindolizidine alkaloids pergularinine and tylophorinidine: the in vitro cytotoxicity of these plant alkaloids and their potential as antimicrobial and anticancer agents, Toxicol. In Vitro 14 (2000) 53–59.
[11] D. Staerk, A.K. Lykkeberg, J. Christensen, B.A. Budnik, F. Abe, J.W. Jaroszewski, In vitro cytotoxic activity of phenanthroindolizidine alkaloids from Cynanchum vincetoxicum and Tylophora tanakae against drug-sensitive and multidrug-resistant cancer cells, J. Nat. Prod. 65 (2002) 1299–1302.
[12] C.W. Yang, W.L. Chen, P.L. Wu, H.Y. Tseng, S.J. Lee, Anti-inflammatory mechanisms of phenanthroindolizidine alkaloids, Mol. Pharmacol. 69 (2006) 749–758.
[13] H.S. Shiah, W. Gao, D.C. Baker, Y.C. Cheng, Inhibition of cell growth and nuclear factor-kappaB activity in pancreatic cancer cell lines by a tylophorine analogue, DCB-3503, Mol. Cancer Ther. 5 (2006) 2484–2493.
[14] L. Wei, A. Brossi, R. Kendall, K.F. Bastow, S.L. Morris-Natschke, Q. Shi, K.H. Lee, Antitumor agents 251: synthesis, cytotoxic evaluation, and structure-activity relationship studies of phenanthrene-based tylophorine derivatives (PBTs) as a new class of antitumor agents, Bioorg. Med. Chem. 14 (2006) 6560–6569.
[15] P.C. John, M. Mews, R. Moore, Cyclin/Cdk complexes: their involvement in cell cycle progression and mitotic division, Protoplasma 216 (2001) 119–142.
[16] M. Arellano, S. Moreno, Regulation of CDK/cyclin complexes during the cell cycle, Int. J. Biochem. Cell Biol. 29 (1997) 559–573.
[17] S. Amin-Hanjani, P. Wadsworth, Inhibition of spindle elongation by taxol, Cell Motil. Cytoskeleton. 20 (1991) 136–144.
[18] M. Suzuki, Y. Hosaka, H. Matsushima, T. Goto, T. Kitamura, K. Kawabe, Butyrolactone I induces cyclin B1 and causes G2/M arrest and skipping of mitosis in human prostate cell lines, Cancer Lett. 138 (1999) 121–130.
[19] S.K. Lee, K.A. Nam, Y.H. Heo, Cytotoxic activity and G2/M cell cycle arrest mediated by antofine, a phenanthroindolizidine alkaloid isolated from Cynanchum paniculatum, Planta Med. 69 (2003) 21–25.
[20] K.T. Yao, H.Y. Zhang, H.C. Zhu, F.X. Wang, G.Y. Li, D.S. Wen, Y.P. Li, C.H. Tsai, R. Glaser, Establishment and characterization of two epithelial tumor cell lines (HNE-1 and HONE-1) latently infected with Epstein-Barr virus and derived from nasopharyngeal carcinomas, Int. J. Cancer 45 (1990) 83–89.
[21] T.H. Chuang, S.J. Lee, C.W. Yang, P.L. Wu, Expedient synthesis and structure-activity relationships of phenanthroindolizidine and phenanthroquinolizidine alkaloids, Org. Biomol. Chem. 4 (2006) 860–867.
[22] H.Y. Tseng, S.H. Wu, W.H. Huang, S.F. Wang, Y.N. Yang, N. Mahindroo, T. Hsu, W.T. Jiaang, S.J. Lee, Benzothiazolium compounds: novel classes of inhibitors that suppress the nitric oxide production in RAW264.7 cells stimulated by LPS/IFNgamma, Bioorg Med Chem Lett 15 (2005) 2027–2032.
[23] J.M. Blanchard, Cyclin A2 transcriptional regulation: modulation of cell cycle control at the G1/S transition by peripheral cues, Biochem. Pharmacol. 60 (2000) 1179–1184.
[24] C. Weiss, D. Faust, I. Schreck, A. Ruff, T. Farwerck, A. Melenberg, S. Schneider, B. Oesch-Bartlomowicz, J. Zatloukalova, J. Vondracek, F. Oesch, C. Dietrich, TCDD deregulates contact inhibition in rat liver oval cells via Ah receptor, JunD and cyclin A, Oncogene 27 (2008) 2198–2207.